Journal of Hazardous Materials 163 (2009) 607–617

Contents lists available at ScienceDirect

Journal of Hazardous Materials

journal homepage: www.elsevier.com/locate/jhazmat

An environmentally friendly process; Adsorption of radionuclide Tl-201 on fibrous waste tea

Hayrettin Eroğlu[a], Sinan Yapici[b,*], Çiğdem Nuhoğlu[c], Erhan Varoğlu[a]

[a] Atatürk Üniversitesi, Araştırma Hastanesi, Nükleer Tıp Ana Bilim Dalı, 25240 Erzurum, Turkey
[b] Atatürk Üniversitesi, Mühendislik Fakültesi, Kimya Mühendisliği Bölümü, 25240 Erzurum, Turkey
[c] Atatürk Üniversitesi, Fen-Edebiyat Fakültesi, Fizik Bölümü, 25240 Erzurum, Turkey

ARTICLE INFO

Article history:
Received 11 March 2008
Received in revised form 6 June 2008
Accepted 3 July 2008
Available online 23 July 2008

Keywords:
Radionuclide
Thallium-201
Adsorption
Bio-sorption
Radioactivity
Waste water

ABSTRACT

This work presents an investigation of the adsorption of the radionuclide of Tl-201 from waste water on the fibrous tea factory waste. The experimental parameters were chosen as temperature, pH, stirring speed, adsorbent dose and nominal particle size in the ranges of 10.0–40.0 °C, 2.0–10.0, 300–720 rpm, 1.0–15.0 g/L and 0.15–0.71 mm, respectively. The most effective parameter on the adsorption yield was found to be pH of the solution. Fourier transforms infrared and electron paramagnetic resonance spectroscopy studies were performed for the characterisation of the adsorption on tea waste. The experimental data were found to be in good agreement with the isotherm models of Freundlich, Halsey, Handerson and Dubinin–Radushkevich. Thermodynamic analysis showed that the values of ΔG and ΔH are negative. It was obtained that the adsorption rate can be represented very well by second-order pseudo homogeneous kinetic model. All the results proved that fibrous tea plant waste makes an excellent adsorbent for Tl-201 radionuclide.

1. Introduction

There are three fundamental ways for the protection from radiation; the application of the rules of time, distance and shielding. Radiation causes very serious biological effects. The radiation from ionised radioactive sources can cause some changes in molecular level in the cell through which they pass, in similar ways to those caused by X, gamma, alpha and beta rays. These changes can cause temporary (curable) or permanent (non-curable) damages depending upon the type, amount and period of suffered radiation. There is no cell which has absolute resistance to radiation [1].

In nuclear medicine, the production of some solid or liquid radioactive wastes is unavoidable; these wastes can have different chemical structures, activities and concentrations. Liquid radioactive wastes can be classified according to their sources, chemical compositions or salt contents [2].

For the intravenous application in nuclear medicine, the sterilised apyrogenic thallium chloride is prepared from thallium-201 formed by degeneration of Pb-201 radionuclide produced by the bombardment of Tl-203 in cyclotron. Tl-201 radionuclide converts to Hg-201 as follow:

$$Tl^{201} \rightarrow Hg^{201} + \text{gamma ray}[135 - 167\text{Kev}(12\%)] + \text{X-ray}[69 - 83\text{Kev}(88\%)] \quad t_{1/2} = 73.1\,\text{h} \tag{1}$$

The discharge of the radionuclides by patient or of the unused radioactive substances as a waste to the environment can cause serious radioactive problems. The precautions to reduce this problem are to keep the liquid wastes in lead tanks and the solid wastes in lead chambers until their radioactivity level reduces to an allowable value to discharge into the environment. This method is expensive, cumbersome and far away being practical and avoiding the harmful effect of radioactivity [3]. Moreover, this method cannot provide a complete shielding for radioactivity besides the tanks or chambers occupy large areas. Finally, the diluted radionuclides are left to the environment before their activity is reduced to a harmless level. In addition to the radioactive contamination, it causes heavy metal contamination and poisoning because radionuclides convert to stable metal ions in their steady states. When they mix with underground water, their harmful effects become unavoidable [1]. Therefore, the removal of these ionised radioactive substances from liquid wastes is of vital importance. There are various ways of removing these ionised species from waste water such as reverse osmosis, ion exchange, precipitation and coagulation. However, these methods are quite expensive and are not so

* Corresponding author. Tel.: +90 442 231 4553; fax: +90 442 231 4544.
E-mail address: syapici@atauni.edu.tr (S. Yapici).

0304-3894/$ – see front matter © 2008 Elsevier B.V. All rights reserved.
doi:10.1016/j.jhazmat.2008.07.076

Nomenclature

B_r	resonance field
C	concentration of adsorbate in the solution at equilibrium ($mg\,L^{-1}$)
E	adsorption free energy ($J\,mol^{-1}$)
E_A	activation energy ($J\,mol^{-1}$)
G	Gibbs free energy ($J\,mol^{-1}$)
H	enthalpy ($J\,mol^{-1}$)
h	Planck constant ($6.626068 \times 10^{-34}\,J\,s$)
k	kinetic rate constant
K	constant related to adsorption capacity ($L\,g^{-1}$)
K_1	constant related to adsorption energy ($mol^2\,kJ^{-2}$)
n	constant related to adsorption intensity
q	adsorbed amount per amount adsorbent at equilibrium ($mg\,g^{-1}$)
R	regression coefficient, ideal gas constant ($8314\,J\,K^{-1}\,mol^{-1}$)
S	entropy ($J\,mol^{-1}\,K^{-1}$)
T	absolute temperature (K)
t	time (min)

Subscript

t	any time
t_0	initial period
e	equilibrium

Greek letters

Δ	change
ε	Polany potential
ν	microwave frequency

effective if the waste contains radionuclides in low concentrations [4]. Therefore, after treatment of the liquid waste with one of the above methods, the waste still contains poisonous materials. The use of sorbents for removing radionuclides has some advantages over the other methods [5]. Many microorganisms such as spores, yeasts, bacteria and sea organisms can adsorb anionic and cationic species in liquid medium [6,7].

To remove radioactive species in liquid medium, an ion exchange process was applied, and Iodine-131 was removed by the use of amberlite as ion exchanger [8]. Clinoptilolite, which is a zeolite, was used to adsorb and successful results were obtained [9]. Cr-51 radionuclide used in nuclear medicine was removed by the use of water plants such as *Eichhornia crassipes*, *Pista* sp., *Nymphea alba*, *Menhta aquatica*, *Ephorbia* sp. and *Lemna minor* as adsorbents [10]. Activated carbon was also used for the adsorption of radionuclides in aqueous medium such as uranium [11] and iodine [12].

The aim of this work is to investigate the adsorption of the radioactive ions of Thallium-201 from waste water by using the fibrous tea factory waste as adsorbent and to study the effect of some experimental parameters on the adsorption yield.

2. Materials and method

2.1. Adsorbent

Solid wastes in large amounts are produced in the factories which process agricultural products. These wastes, sometimes, occupy large areas in the operation site of factories, creating some difficulties in the regular operation of the factories. Approximately, 20,000 tonnes tea waste is produced in the official tea factories in Turkey. When the private sector is considered, this amount rises to about 30,000 tonnes [13]. The tea factory waste used as adsorbent was provided from Cumhuriyet tea plant located in Rize in Black Sea Region of Turkey. There are two types of the tea factory waste in Cumhuriyet tea plant such as subjacent of sieve and chimney. The fibrous tea factory waste (FTFW) of the chimney subjacent was used in this research. The solid waste first was ground and then sieved to obtain desired particle size fractions.

Table 1
Some properties of waste tea used in experiments

Bulk density (g/cm^3)	0.119
Particle size (mm)	0.212–0.150
BET surface area (m^2/g)	0.702

Some properties of the tea factory waste are presented in Table 1. Prior to the experiments, other soluble contaminants and coloured components were removed from the waste tea by washing it with distilled water for a few times until a colourless filtrate of the washing water was spectrometrically observed at room temperature. The decolourized and cleaned tea waste was dried at room temperature for a few days, and then used in the adsorption experiments.

2.2. Experimental system

The system shown in Fig. 1 was employed in the adsorption experiments. In the design of this experimental system, all the necessary safety considerations were taken into account so that the person who carries out the experiments will expose to radioactivity at possible minimum level. A 1000-mL jacketed vessel was used as the adsorption medium. A mechanical mixer was attached to the system to stir the content of the vessel during the adsorption process. A circulating bath was employed to keep the adsorption medium at constant temperature by circulating the cooling/heating fluid through the jacket. A master flex pump was used to circulate the aqueous solution through the radiation dosimeter to measure automatically the radioactivity of the solution. The circulation of the adsorption solid together with the solution was avoided by using a suitable filter, which does not adsorb the radioactive substance, just at the outlet of the solution from the vessel. All the necessary precautions were taken for an accurate measurement with the dosimeter. The experimental readings of digital screens were recorded by a video camera to minimize the involvement of the researcher with the radioactive medium.

The experimental parameters were chosen as temperature, pH, stirring speed, adsorbent dose and nominal particle size. The ranges of these parameters are given in Table 2. When the effect of one parameter on the adsorption was investigated, the values of the

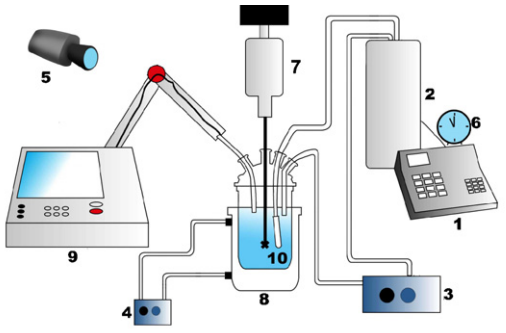

1. Radioactivity dosimeter
2. Radioactivity reading chamber
3. Pump
4. Circulating bath
5. Video camera
6. Clock
7. Mechanical stirrer
8. Jacketed adsorption vessel
9. pH meter
10. Filter

Fig. 1. Experimental system.

Table 2
Experimental parameters and their range

pH	Adsorbent dose (g/L)	Stirring speed (rpm)	Particle size (mm)	Temperature (°C)
2.0–10.0	1.0–15.0	300–720	0.15–0.71	10.0–40.0

Table 3
Zeta potentials of tea waste at different pH values

pH	4.0	6.0	7.0	8.0	10.0
Zeta potential (mV)	−41.8	−43.8	−48.9	−56.4	−78.4

other parameters were kept constant at 7.0 for pH, 0.150–0.212 mm for particle size, 10 g/L for adsorbent dose, 20 °C for temperature and 600 rpm for stirring speed.

To determine the surface charge of the tea plant waste, the zeta potentials of the particles were determined by using a zeta potential meter at different pH values. This is determined by the measurement of particle velocities in an electrical area. As seen from Table 3, increasing pH increases the zeta potential of FTFW particles. At neutral conditions, the surface charge has a negative value of −48.9 mV. Increasing pH of the solution increases the concentrations of OH^-; these OH^- ions increase the negative charge of the surface by neutralising the positive groups on the surface. In the case of decreasing pH, the increasing H^+ ions decreases surface negative charge by affecting the negative groups on the surface. Since Tl-201 ion has an electrical charge of +1, increasing the surface negative charge increases the bio-sorption yield due to electrical forces.

2.3. Preparation of radioactive solution

Monrol made TlCl solution having 95% radiochemical purity, a specific activity of 2782 GBq and 0.9% NaCl was used to prepare the radioactive solution by taking into consideration the production date and decaying rate. The solution was provided as fresh as possible. This solution was added into the aqueous medium having an adjusted temperature, stirring speed, particle size, adsorbent dose and an initial pH value to obtain a 500 mL-solution with an initial radionuclide concentration of approximately 800 μCi, which resembles the average radioactive value of the aqueous waste. Since to increase the concentration of the radioactive species is not a safe way due to high radioactivity, the equilibrium was changed by using different amount of the adsorbent while keeping the initial amount of the radioactive species at this constant initial value when the adsorption isotherms were studied.

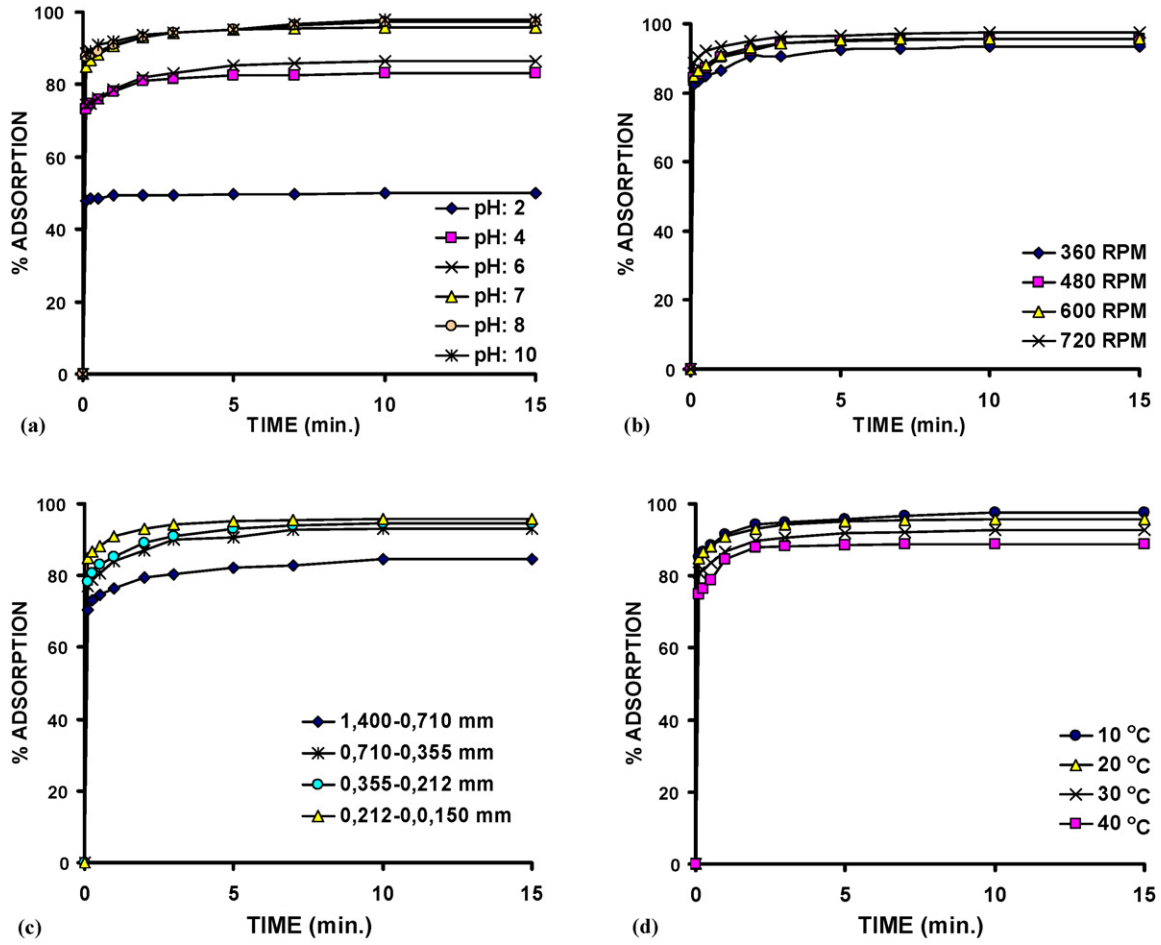

Fig. 2. Effect of experimental parameters on adsorption: (a) effect of pH; (b) effect of stirring speed; (c) effect of particle size; (d) effect of temperature.

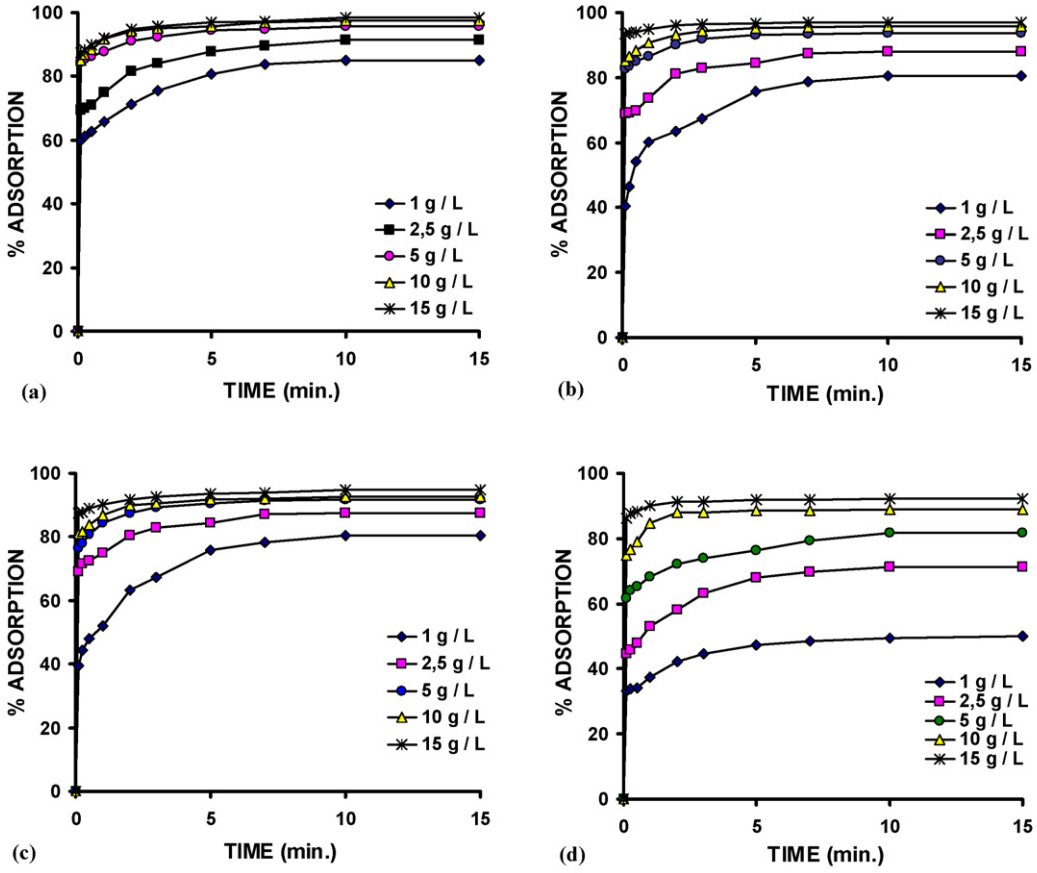

Fig. 3. Adsorption of Tl-201 at different temperatures and different adsorbent doses: (a) 10 °C; (b) 20 °C; (c) 30 °C; (d) 40 °C.

2.4. FTIR and EPR analysis

Fourier transforms infrared (FTIR) and electron paramagnetic resonance (EPR) spectroscopy studies were performed for the characterisation of the adsorption mechanism of FTFW. The FTIR spectra were obtained employing a PerkinElmer Spectrum One FTIR spectrometer and the EPR spectra using a Varian E104 EPR spectrometer with x-band spectrometer at 9.53 GHz with.

3. Results and discussion

Tl-201, which is one of the most used radionuclides in nuclear medicine, was removed from aqueous medium by adsorption using tea plant wastes as adsorbent. The effects of the chosen parameters on the adsorption process were investigated in a batch process to determine the process conditions. The results are submitted in graphs in Fig. 2.

3.1. Effect of pH

To investigate the effect of pH on the adsorption process, the values of pH were chosen as 2.0, 4.0, 6.0, 7.0, 8.0 and 10.0. The change of the adsorbed percentage of Tl-201 with pH is given in Fig. 2(a) as a function of the adsorption period. As seen from the figure, the increasing pH increased adsorption of Tl-201 up to pH 7.0, and after this value almost no change in the adsorption percentage was observed with increasing pH value. At pH 7.0, approximately 97.8% of the initial amount of Tl-201 was adsorbed in 10 min while only about 49.4% of Tl-201 was removed at pH 2.0 in the same period. This can be explained by the increase of the negative charge of the surface potential of FTFW with increasing pH as shown in Table 3. The zeta potential of the adsorbent reduces from 0.0 mV at pH 2.0 to −48.9 mV at pH 7.0. This causes an increase in the adsorption of the positively charged Tl-201 radionuclide with increasing pH. Further decrease in the zeta potential up to −78.4 at pH 10.0 does not cause any increase in the adsorption percentage.

3.2. Effect of stirring speed

For the investigation of the effect of stirring speed on the adsorption of Tl-201, the stirring speed values were chosen as 360, 480, 600 and 720 rpm. The effect of the stirring speed on the adsorption process is presented in Fig. 2(b) as a function of time. Although no pronounced effect of the stirring speed was observed, it can be said that the adsorption percentage slightly increased with the increase in the stirring speed. In 10 min of the adsorption period, the adsorption percentage is 97.5% at 720 rpm while it is 93.4% at 320 rpm. This small change can be explained by the decrease of the liquid film thickness with increasing stirring speed; this results in a slight increase in the arrival rate of Tl-201 ions to the surface of the adsorbent. The small change also shows that the adsorption rate is not controlled by diffusion of Tl-210 from the film layer around the particles.

3.3. Effect of adsorbent particle size

To investigate the effect of the adsorbent particle size on the adsorption process, the particle sizes were taken as the nominal sizes of 1.40–0.71, 0.71–0.355, 0.355–0.212 and 0.212–0.150 mm. The experimental results are presented in Fig. 2(c) in the plot of the

Table 4
Adsorption percentage at equilibrium for adsorbent doses of 1 and 15 at different temperatures

Temperature (°C)	Adsorbent dose (g/L)	Adsorption yield (% ads.)
10	1.0	85.1
	15.0	98.4
20	1.0	80.4
	15.0	97.0
30	1.0	80.3
	15.0	94.7
40	1.0	49.3
	15.0	92.3

adsorption percentage versus time at different particle size values. No emphasized effect of the particle size was also observed. However, it can be said that increasing particle size resulted in a small decrease in the adsorption percentage. For example, for an adsorption process of 10 min, 97.1% of the initial Tl-201 was removed at a particle size of 0.150–0.212 mm while 93.2% was adsorbed at the particle size of 0.355–0.710 mm. This can be explained by the increase in the outer surface area per weight of the solid and the decrease in the nominal transfer distance into the particle with the decrease of the particle size.

3.4. Effect of temperature

The effect of the temperature on the adsorption was investigated for the temperatures of 10, 20, 30 and 40 °C. The plot of the adsorption percentage versus time is given in Fig. 2(d) for different temperatures. Increasing temperature decreased the adsorption percentage; the highest removal percentage was obtained at 10 °C. For the adsorption period of 10 min, approximately 97.5% of the initial Tl-201 was removed at 10 °C while 88.7% was adsorbed at 40 °C. The effect of the temperature on the process is slightly more pronounced than the stirring speed and the particle size and less than pH. This behaviour can be an indication that the adsorption process is a physical and exothermic process.

3.5. Effect of adsorbent dose

To see the effect of the adsorbent dose on the adsorption process some adsorption experiments were carried out at the different adsorbent dose values of 1.0, 2.5, 5.0, 10.0 and 15.0 g solid/L solution while keeping the value of the other parameters at their constant values given in Section 2.2. To study the adsorption isotherms these experiments were carried out at four different temperatures as shown in Fig. 3. All the plots for different temperatures showed similar behaviour; increasing adsorbent dose increased adsorption percentage. For the adsorption at 20 °C the removal percentage of Tl-201 versus the adsorption period is given for different adsorbent doses as seen in Fig. 3(b). The adsorption increased decreased with increasing adsorbent dose, and the maximum yield was obtained at 15 g/L. However, the effect of this parameter diminished with its increasing value. The removal percentage is 97.0 for 15 g/L, and 80.4 for 1 g/L for an adsorption period of 10 min. The increase in the adsorption with the increase in the adsorbent dose can be explained by the increase of the available adsorption area for a constant initial value of Tl-201 concentration.

To see the effect of the temperature and the adsorbent dose on the adsorption, the adsorption percentages are submitted in Table 4 for different ratios and temperatures for an adsorption period of 10 min corresponding to the equilibrium values. As seen from Table 4, with the increase of the temperature from 10 to 40 °C the adsorption percentage decreased from 85.1% to 49.3% for an adsorbent dose of 1.0 while it decreased from 98.4% to 92.3% for the dose of 15.0.

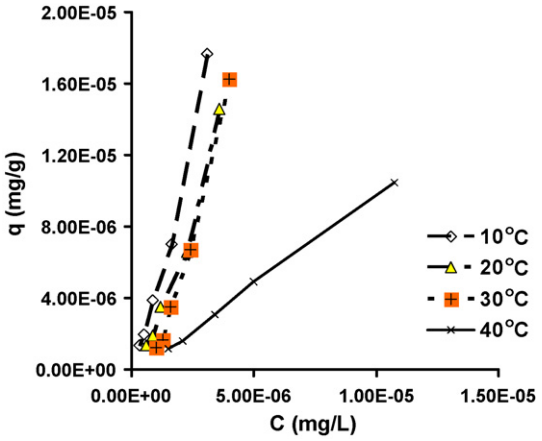

Fig. 4. Adsorption isotherms.

3.6. Adsorption isotherms

Adsorption isotherms, which are called equilibrium lines, relate the adsorbed amount on the adsorbent to the non-adsorbed amount in the fluid bulk at equilibrium for a given temperature. These isotherms exhibit different behaviours in a wide variety. The adsorption isotherms were studied by using the data in Fig. 3(a), and the isotherms are given graphically in Fig. 4. The models, which show good agreement with experimental results, are submitted below.

Freundlich model:

$$q = KC^{1/n} \tag{2}$$

Halsey model:

$$\ln q = \left[\left(\frac{1}{n}\right)\ln K\right] - \left(\frac{1}{n}\right)\ln\left[\ln\left(\frac{1}{C}\right)\right] \tag{3}$$

Henderson model:

$$\ln q = \left(\frac{1}{n}\right)\ln[-\ln(1-C)] - \left(\frac{1}{n}\right)\ln K \tag{4}$$

Dubinin–Radushkevich (D–R) model:

$$\ln q = \ln q_{\mathrm{m}} + K_1\varepsilon^2 \tag{5}$$

$$\varepsilon = RT\ln\left(1+\frac{1}{C_{\mathrm{e}}}\right) \tag{6}$$

$$E = (2K_1)^{-0.5} \tag{7}$$

where k, n, K, K_1 in these equations are constants which are dependent on temperature, adsorbent type and adsorbate.All the above models are based on that the adsorption is multilayered and the active sites have heterogeneous energy distribution. Therefore, the fit of the experimental data to the above models shows that the adsorption process has a multilayered character and the adsorption surface is not uniform and possibly has a heterogeneous structure [14–16]. Statistically these models well represent the experimental data with R^2 values higher than 0.9881. The fit of the data with Freundlich isotherm is graphically submitted in Fig. 5. Table 5 shows that all the values of the constants of all the models given above exhibited a regular behaviour, continuously increasing or decreasing, with temperature up to 30 °C. However, at 40 °C, they exhibited just opposite of their regular behaviour which they had up to this temperature. This can be attributed to possibility that the chemical

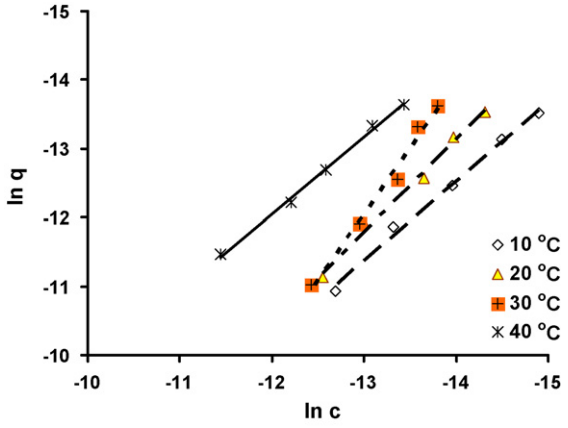

Fig. 5. Fit of data to adsorption isotherm models.

adsorption starts to play an appreciable role in the process after this temperature. The high change of K values of Freundlich isotherm can also be explained with this attitude of the process.

3.7. FTIR and EPR analysis

FTIR and EPR spectroscopy studies were used to characterize the reaction mechanism of FTFW. These spectra were obtained using PerkinElmer Spectrum One model FTIR spectrometer, and an x-band EPR spectrometer at 9.53 GHz by Varian E104 EPR spectrometer, respectively. The FTIR spectra of FTFW before and after adsorption are shown in Fig. 6.

3.7.1. Adsorption mechanism determined by FTIR and EPR analysis

Before recording the FTIR spectra of the thallium loading FTFW, the spectrum of the FTFW alone was recorded in order to determine the main functional groups of FTFW participate in the thallium adsorption. The FTIR spectroscopic characteristics from the FTIR

Table 5
Model constants and regression coefficients of isotherm models

Isotherm model	Temperature (°C)			
	10 Constants and regr. coefficient	20 Constants and regr. coefficient	30 Constants and regr. coefficient	40 Constants and regr. coefficient
Freundlich	$n = 0.871$ $K = 34.74$ $R^2 = 0.9900$	$n = 0.721$ $K = 268.27$ $R^2 = 0.9850$	$n = 0.519$ $K = 444{,}631$ $R^2 = 0.9965$	$n = 0.9$ $K = 3.82$ $R^2 = 0.9936$
Halsey	$n = 0.0625$ $K = 6.38$ $R^2 = 0.9881$	$n = 0.0567$ $K = 6.63$ $R^2 = 0.99$	$n = 0.0411$ $K = 7.91$ $R^2 = 0.9963$	$n = 0.0717$ $K = 1.62$ $R^2 = 0.9925$
Henderson	$n = 0.871$ $K = 0.0455$ $R^2 = 0.9900$	$n = 0.747$ $K = 0.0153$ $R^2 = 0.985$	$n = 0.519$ $K = 0.00118$ $R^2 = 0.9965$	$n = 0.896$ $K = 0.301$ $R^2 = 0.9936$
D–R	$K_1 = 7 \times 10^{-9}$ $q_m = 0.0127$ $E = 23904.6$ $R^2 = 0.9895$	$K_1 = 8 \times 10^{-9}$ $q_m = 0.034$ $E = 22360.6$ $R^2 = 0.9870$	$K_1 = 10 \times 10^{-9}$ $q_m = 1.147$ $E = 20{,}000$ $R^2 = 0.9976$	$K_1 = 7 \times 10^{-9}$ $q_m = 0.00382$ $E = 23904.4$ $R^2 = 0.9904$

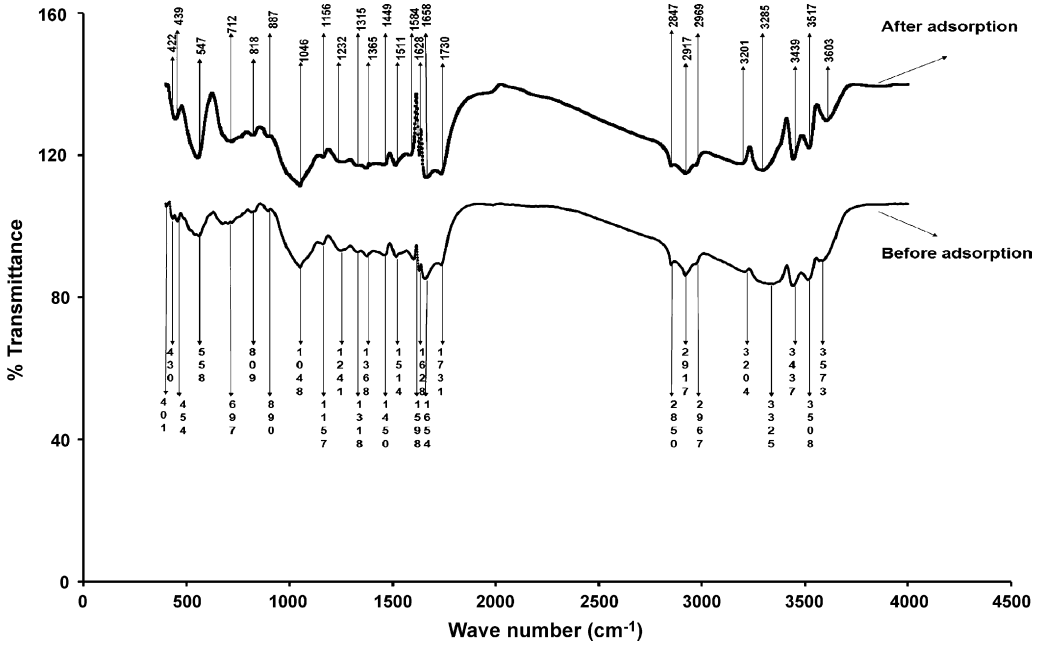

Fig. 6. FTIR spectra of waste tea before and after adsorption.

Table 6
FTIR spectral characteristics of tea factory waste before and after adsorption

IR peak	Frequency (cm^{-1})			Assignment
	Before adsorption	After adsorption	Differences	
1	3573	3603	+30	Bonded —OH groups
2	3508	3517	+9	Bonded —OH groups
3	3437	3439	+2	Bonded —OH groups
4	3325	3285	−40	Bonded —OH groups
5	3204	3201	−3	N—H stretching
6	2967	2969	+2	Aliphatic C—H group
7	2917	2917	0	Aliphatic C—H group
8	2850	2847	−3	Aliphatic C—H group
9	1731	1730	−1	C=O stretching
10	1654	1658	−4	C=O stretching
11	1628	1628	0	C=O stretching
12	1598	1584	−14	Secondary amine group
13	1514	1511	−3	Secondary amine group
14	1450	1449	−1	Symmetric bending of CH_3
15	1368	1365	−3	Symmetric bending of CH_3
16	1318	1315	−3	Symmetric bending of CH_3
17	1241	1232	−9	—SO_3 stretching
18	1157	1156	−1	C=O stretching of ether groups
19	1048	1046	−2	C=O stretching
20	890	887	−3	Aromatic —CH stretching
21	809	818	+9	Aromatic –CH stretching
22	697	712	+15	—CN stretching
23	558	547	−11	—C—C— group
24	454	439	−15	Amine group
25	430	422	−8	Amine group
26	401	Disappeared	Unknown	Amine group

Table 7
Values of ΔG at different temperatures

Temperature (K)	283	293	303	313
ΔG (J/mol)	−8636.0	−7575.0	−6469.3	−5377.9

spectra in Fig. 6 are shown in Table 6. This figure shows that FTFW represents complex adsorption band characteristics including the 26 adsorption bands, indicating the complex nature of the bio-sorbent.

As seen in Table 7, 13 significant band decreases of the functional groups on the bio-sorbent were detected at the bands of 3325, 3196, 2917, 1731, 1588, 1514, 1450, 1368, 1157, 1048, 809, 558 and 454 cm^{-1}. The spectral analysis before and after thallium adsorption indicated that especially the bonded —OH groups, secondary amine group, N—H stretching, amine group, C=O stretching, aliphatic C–H group, symmetric bending of CH_3, C—O stretching of ether groups, —C—C— and amine group were especially involved in thallium adsorption [17,18]. The 13 adsorption bands participating in the bio-sorption indicated that FTFW is an excellent bio-sorbent for the removal of thallium and thus the adsorption time is very fast. The different functional groups have a high affinity towards Tl—Cl so that they can complex the metal ions [19]. These properties of the FTFW can also make this material suitable for continuous flow treatment systems [20].

EPR spectroscopy is a technique applicable only to the systems with net electron spin angular momentum(S); nevertheless, a respectable number of systems fulfil this condition. These include free radicals in the solid, liquid or gaseous states, some point defects (localized crystal imperfections) in solids, bio-radicals, systems in the triplet state (two unpaired electrons), systems with three or more unpaired electrons, most transition-metal ions and rare-earth ions [21]. The flipping of spins induced in a paramagnetic system embedded in a static magnetic field by the absorption of the electromagnetic radiation is the physical principle behind the EPR technique. For a system with a spin $S = 1/2$, e.g. a free electron or a radical, there are two energy levels corresponding to the spin parallel and non-parallel to the static magnetic field and the possible values of M_S are $+1/2$ and $-1/2$. The latter has the character of having lowest energy [22].

EPR can be applied to the investigation of metal-charged biomasses. For this aim, the main information provided by this technique are the chemical identity, valence states and relative concentration of the metals involved in the bio-sorption processes [23]. In the early researches, the adsorption data were combined with EPR spectroscopy to obtain structural information about the metal binding and estimate of adsorption mechanism [22–25]. By the analysis of the EPR spectra, it is also possible to get an insight about the local environment of the transition metal ion in the biomass, i.e. the site symmetry and the electronic density at neighbouring

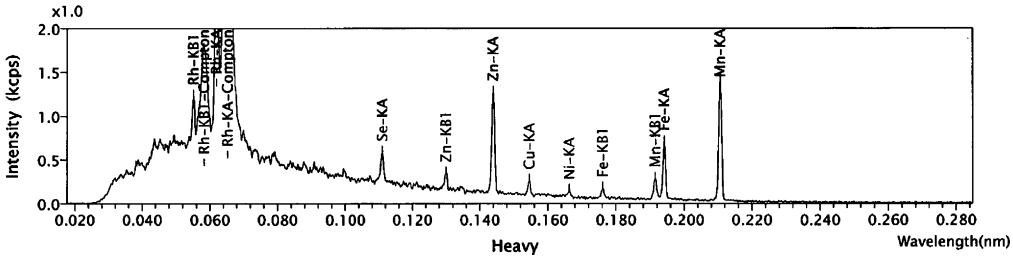

Fig. 7. XRF spectra of waste tea after adsorption.

nuclei [22]. In this research, in order to compare the natural and thallium binding FTFW and estimate mechanism of thallium ion bio-sorption, the EPR spectra were taken from the alone and thallium loading. The EPR spectra before and after adsorption by FTFW are shown in Fig. 8. It was shown in this figure that these spectra are two typical EPR signals belonging to Mn^{2+} and SO_3^- ion spectra. The bio-sorption of thallium by FTFW is investigated by using Mn^{2+} and SO_3^- spectra. These findings were confirmed with XRF analysis. As seen in Fig. 7, XRF analysis indicated that some of determining components of the FTFW are carbon, oxygen, manganese and sulphur in the amounts of 57.458%, 37.281%, 0.0731% and 0.1652% (w/w), respectively.

By comparing the natural and thallium loaded EPR signal, it was observed that the amplitude of EPR signals decreased after adsorption. The broad EPR lines stem from strong dipolar interactions of their unpaired magnetic moments. The capture of thallium by biomasses is also observed by using EPR spectroscopy to study thallium adsorption on FTFW samples, which were measured using an x-band (9.535 GHz) EPR spectrometer with modulation of magnetic field of 100 kHz. The microwave frequency was recorded, and EPR spectra were measured with attention of 10 dB to avoid microwave saturation of resonance absorption curves. EPR studies were carried out via Mn^{2+} and SO_3^- spectra since natural FTFW represents only these spectra before adsorption. With $S = 5/2$ (in the high-spin case), $I = 5/2$ for Mn^{2+} with 100% natural abundance. g-Factor was calculated from resonance conditions as seen in follows:

$$g = \frac{h\nu}{\beta B_r} \tag{8}$$

Seven lines were observed in these resonance absorption curves in Fig. 8. Mn^{2+} ion is responsible for six of these EPR components. EPR lines resolved hyperfine structures are characteristics of Mn^{2+}. SO_3^- ion is responsible for a very intense resonance line in band centred, $I = 1/2$ for SO_3^- ion with natural abundance (>97.7%) [31]. EPR spectra at about 3555 G ($g = 1.916$), 3445 G ($g = 1.977$), 3375 G ($g = 2.018$), 3340 G ($g = 2.039$), 3230 G ($g = 2.109$), 3145 G ($g = 2.166$) and 3075 G ($g = 2.215$). Hyperfine splitting constants are 125, 65, 30, 110, 90 and 60 G, respectively. Average g value is 2.062.

It can be seen from Fig. 8 in the TlCl-tea after adsorption 3565 G ($g = 1.910$), 3445 G ($g = 1.997$), 3365 G ($g = 2.024$), 3335 G ($g = 2.042$), 3250 G ($g = 2.096$), 3160 G ($g = 2.155$) and 3065 G ($g = 2.222$). Hyperfine splitting constants are 120, 85, 35, 80, 95 and 100 G, respectively. Average g value is 2.063. The g-value close to 2 confirms that the free radicals or transition metal ions do have $g = 2$, but there are also systems which show marked deviations from this value [21]. Considerable changes of EPR spectra of Mn^{2+} and SO_3^- ion were observed after adsorption. Remarkable Tl-Cl dependences

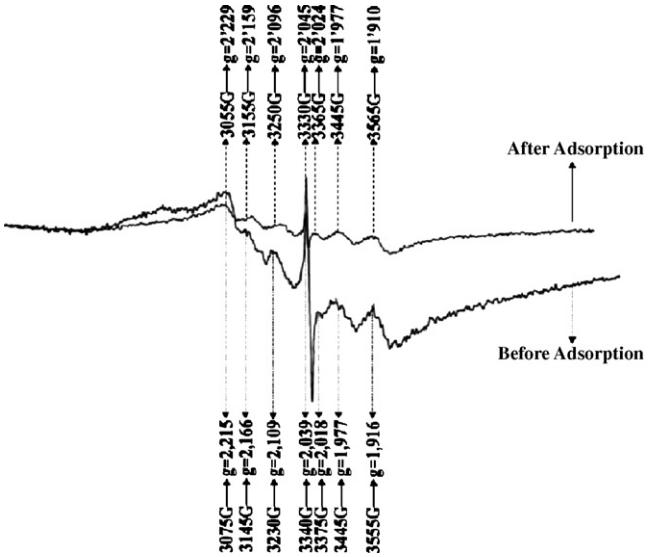

Fig. 8. EPR spectra of FTFW were measured at room temperature (25 ± 2 °C) with a microwave frequency of 9.535 GHz.

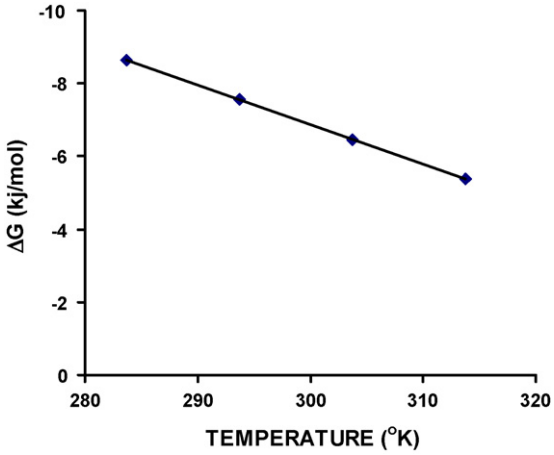

Fig. 9. ΔG versus T plot.

of the line width and line intensity in EPR spectra of Mn^{2+} and SO_3^- ion were observed. Some of Mn^{2+} and SO_3^- ions are bounded after adsorption because line intensities decrease. These results indicated that the bio-sorption processes may be carried out partially

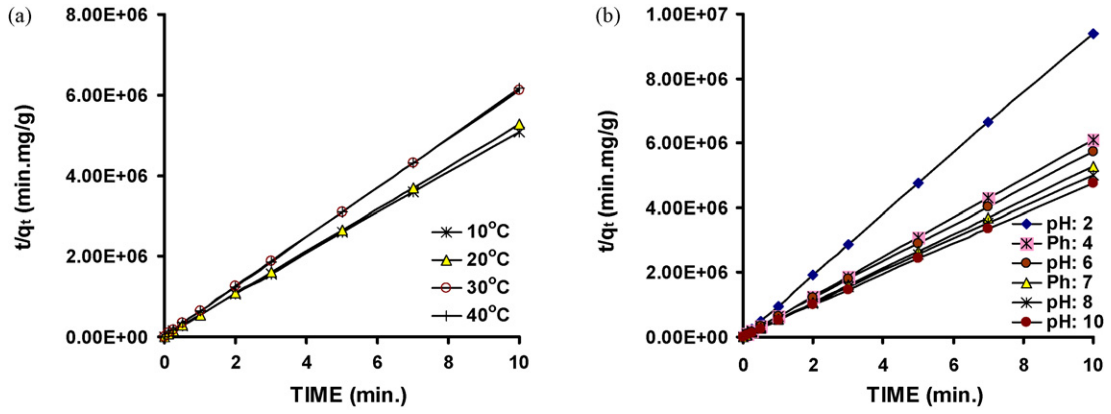

Fig. 10. Agreement of experimental data with pseudo second-order kinetic model.

Table 8
Values of experimental and theoretical q, kinetic constants and statistical R^2

Parameters		$q_{exp} \times 10^6$ (mg g^{-1})	$q_{thr} \times 10^6$ (mg g^{-1})	$k \times 10^{-6}$ (mg g^{-2} min^{-1})	$h \times 10^5$ (mg g^{-1} min^{-1})	R^2
Temperature (°C)	10	1.9661	1.9654	11.026	4.2622	0.9999
	20	1.9031	1.8987	15.118	5.4755	1
	30	1.6375	1.6359	13.201	3.5398	0.9999
	40	1.6293	1.623	18.801	4.9910	1
pH	2	1.0612	1.0633	58.563	6.5950	1
	4	1.6428	1.6402	16.307	4.4010	1
	6	1.7504	1.7464	8.703	2.6665	0.9998
	7	1.9031	1.8987	15.118	5.4755	1
	8	1.9963	1.9978	10.243	4.0821	0.9999
	10	2.0995	2.1042	97.677	4.3055	0.9998

via chemi-sorption involving valence forces through sharing or exchange of electrons between FTFW and Tl-Cl [26]. This occurrence was confirmed FTIR analysis as seen in Table 7. The fast bio-sorption kinetics observed is typical for bio-sorption of metals involving no energy-mediated reactions, where metal removal from solution is due to physicochemical interactions between biomass and metal solution [27].

3.8. Thermodynamic analysis

For adsorption process, Gibbs free energy can be written as follow:

$$\Delta G = -RT \ln k \tag{9}$$

where $k = (q/C)_{eq}$

The following relation, which relates Gibbs free energy change to the enthalpy and entropy change, can also be written:

$$\Delta G = \Delta H - T\Delta S \tag{10}$$

Using the experimental data together with (Eq. (9)), the calculated values of ΔG at different temperatures are given in Table 7. From the plot of ΔG versus T shown in Fig. 9, ΔH and ΔS were calculated [28]. The values were found to be $\Delta H = -39{,}516$ J/mol and $\Delta S = -108.8$ J/mol K. The negative values of ΔG show that the adsorption process can proceed spontaneously. The negative value of ΔH confirms that this adsorption process is exothermic character and increasing temperature affects inversely the process.

3.9. Adsorption kinetics

The models for the adsorption kinetics are related to the removal ratio of the adsorbate. Therefore, these models are important in the planning of the recovery process by adsorption. When one studies the behaviour of the adsorption with the change of the parameters, submitted before in Fig. 2(a)–(d), it can be seen that the adsorption is a rapid process, and the most effective parameter is the initial pH of the solution, which is related to the surface charge, and then the adsorption dose. There are no pronounced effect of temperature, stirring speed and particle size. Therefore, the process cannot be controlled specially only one of the mechanisms of diffusion through film layer, surface sorption or diffusion through the pores. So the conclusion in the preceding section is confirmed; the mechanism which governs the process is probably a combination of all these mechanisms. However, the kinetic models were tested and it was found that the process fitted to the pseudo second-order kinetic model. For an adsorption process which fits to the pseudo second-order kinetic model the equation can be given as follows [29]:

$$\left(\frac{dq_t}{dt}\right) = k(q - q_t)^2 \tag{11}$$

The integration and rearrangement of this equation between the boundary conditions gives the following relation:

$$\frac{t}{q_t} = \frac{1}{kq^2} + + \left(\frac{1}{q}\right) t \tag{12}$$

where $h = kq^2$ is the initial adsorption rate. The plot of t versus t/q_t should give a straight line if the process fits to the pseudo second-order rate model. The experimental data showed a good agreement with pseudo second-order model as shown in Fig. 10(a) for different temperatures and in Fig. 10(b) for different pH values. The R^2 values for these plots are very high, which are between 0.9998 and 1.0. Table 8 also shows the excellent agreement between the experimental and calculated values.

Fast adsorption rate and the increase of the adsorption percentage with increasing negative surface charge of FTFW and decreasing temperature can also be a clue that this adsorption process has mainly physical character. The activation energy can also show whether the process is governed by physical or chemical mechanism. Arrhenius equation is expressed in the following form:

$$k = k_0 \exp\left(\frac{-E_A}{RT}\right) \tag{13}$$

where k is rate constant, k_0 Arrhenius constant and E_A is the activation energy. The activation energy can be calculated graphically from the plot of $\ln k$ versus $1/T$, as shown in Fig. 11. The activation energy was found to be 10.823 kJ/mol; this low value also confirms that the process is not certainly governed by surface chemical reaction [29]. Although this value lies in the range of 8–22 kJ/mol K for diffusion-controlled process, it is still thought that the process is governed by combined effect of different mechanisms since no emphasized effect of stirring speed, which is a clear indication of diffusion-controlled process, was observed.

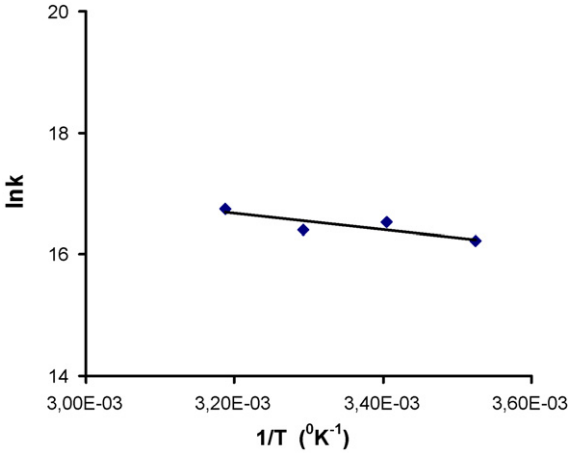

Fig. 11. $\ln k$ versus $1/T$ plot for evaluation of activation energy.

As a result, the Freundlich, the Halsey, the Henderson and D–R isotherm regression coefficient values (R^2) > 0.98 implies that the surface of FTFW is made up of heterogeneous and multilayer bio-sorption patches. For all the ranges studied here, the standard Gibbs free energy (ΔG°) values and the ΔH° parameter which were found out negative indicated thermodynamically feasible, spontaneous and exothermic nature of the bio-sorption. The negative ΔS° value implies a stable arrangement of thallium on FTFW biomass surface and the adsorbed complex of thallium on FTFW is in a more ordered form [30,31]. The FTIR adsorption bands indicated that the 13 adsorption bands participating in bio-sorption are more than other bio-sorbents. EPR studies indicated that the bio-sorption is due to physicochemical interactions between biomass and metal solution.

4. Conclusion

In this work a radionuclide of Tl-201 in a liquid waste was adsorbed on a bio-sorbent which is a solid waste from a tea factory. The results for the adsorption Tl-201 on FTFW showed that:

- FTFW is an excellent adsorbent and it provides a rapid adsorption process. The process reached to equilibrium in about 10 min, and approximately 98% of Tl-201 in the solution was adsorbed.
- The most effective parameter was found to be pH of the solution and then adsorption dose. Increasing temperature had a small decreasing effect on the adsorption yield and stirring speed had a slight increasing effect.
- It was determined that the best laboratory conditions for the adsorption process are 7.0 for pH, 0.150–0.212 mm for particle size, 15 g/L for adsorbent dose, 10 °C for temperature and 600 rpm for stirring speed. Lower stirring speeds and ambient temperature can be preferred for economical reasons.
- FTIR and EPR results indicated that the bio-sorption mechanism of thallium ions onto FTFW have a complex nature with more than one or even two mechanisms, exhibiting a complex mechanism having 13 adsorption band involved in bio-sorption, and has mainly physical character. The good agreement of the experimental equilibrium values with the isotherm models of Freundlich, Halsey, Handerson and D–R confirmed heterogeneous and multilayer bio-sorption patches.
- Negative values of ΔG shows that the adsorption process can proceed spontaneously, and the negative value of ΔH confirms that this adsorption process is of exothermic character.
- It was also concluded that the process rate is controlled by a combination of different mechanisms, and the rate of the process can be represented very well by the pseudo second-order kinetic model.

This process can eliminate the expensive and cumbersome method for handling the radioactive liquid wastes. In the present application, the waste is kept in the closed lead tanks for between 8 and 10 weeks until it decays to the allowable minimum radiation limit to discharge to the environment. According to the regulations of The Republic of Turkey, the allowed concentration for discharging Tl-201 is about 4 μCi. However, since Tl-201 converts Hg, which is one of the most poisonous heavy metals, dumping the waste after even after reaching to allowable radiation limit is still harmful. It is possible to adsorb approximately 98% of Tl-201 in 1 m^3 liquid waste onto 15 kg adsorbent in 10 min, which corresponds to almost allowable limits for discharging to the environments. The solid waste with adsorbed radionuclide can be easily and practically stored in small lead cans until the radiation decays to the harmless level, and then the adsorbed metal can be recovered using a suitable method. For more practical application, further study is being planned to carry out the process in a packed bed composed of cylindrical lead cartridges filled with FTFW.

Acknowledgement

The financial support of Atatürk University for the project BAP-2003/372 is highly appreciated.

References

[1] A. Görpe, S. Cantez, Pratik Nükleer Tıp, İstanbul Tıp Fakültesi Vakfı, İstanbul, 1992, pp. 1–42.
[2] D.V. Marinin, G.N. Brown, Studies of sorbent/ion-exchange materials fort he removal of radioactive strontium from liquid radioactive waste and high hardness groundwasters, Waste Manag. 205 (2000) 545–553.
[3] C.B. Sampson, Textbook of Radiopharmacy Theory and Practice, Gordon and Breach Science Publishers, 1999, pp. 125–244.
[4] J.G. Dean, F.L. Bosqui, K.H. Lanoutte, Removing heavy metals from waste waters, Environ. Sci. Tech. 6 (1972) 518–524.
[5] B. Volesky, Biosorption and biosorbents, in: Biosorption of Heavy Metals, CRP Press, Boca Raton, FL, 1990, pp. 3–43.
[6] B. Volesky, Z.R. Holan, Biosorption of heavy metals, Biotech. Prog. 3 (1995) 235–250.
[7] B. Volesky, H.A. May-Philips, Biosorption of heavy metals by *Saccharomyces cerevisiae*, Microbiol. Biotechnol. 42 (1995) 797–806.
[8] E.İ. Medine, Hasta İyonunun I-131'in Amberlit Anyon Değiştirici Reçine ile Tutulması, Ege Üniversitesi Fen Bilimleri Enstitüsü, Nükleer Bilimler Anabilim Dalı Turkey, 2003.
[9] S. Akyıl, Uranyumun Ayrılmasında Kompozit iyon değiştiricilerin Geliştirilmesi ve Çeşitli Uygulama Alanlarının incelenmesi, Ege Üniversitesi Fen Bilimleri Enstitüsü, Nükleer Bilimler Anabilim Dali, Turkey, 1996.
[10] S.T. Taner, Z. Demire, Z. Üst, Medikal Alanda Ortaya Çıkan Cr-51 Atıkları için Kullanilabilecek Biyolojik Kökenli Bir Adsorban Teklifi, Ege Üniversitesi Fen Bilimleri Enstitüsü, Nükleer Bilimler Anabilim Dalı, Turkey, 2003.
[11] C. Kütahyalı, Mangal Kömüründen Üretilen Aktif Karbon Kullanılarak Uranyumun Selektif Adsorpsiyonunun ve Uygulama Alanlarının İncelenmesi, Ege Üniversitesi Fen Bilimleri Enstitüsü, Nükleer Bilimler Anabilim Dalı, Turkey, 2002.
[12] P.K. Sinha, K.B. Lal, J. Ahmed, Removal of radioiodine from liquid effluents, Pergamon, Waste Manag. 17 (1997) 33–37.
[13] B. Kacar, Çayın Biyokimyası ve İşlenme Teknolojisi, Çay İşletmeleri Genel Müdürlüğü Yayını, DSİ Matbaası, Ankara, 1987, p. 329.
[14] H.M. Jnr, A.I. Spiff, Equilibrium sorption study Of Al^{3+}, Co^{2+} and Ag^{+} in aqueous solutions by fluted Pumpkin (Telfairia Occidentalis HOOK f) waste biomass, Acta Chim. Slov. 52 (2005) 174–181.
[15] S. Karaca, A. Gürses, M. Ejder, M. Açıkyıldız, Adsorptive removal of phosphate from aqueous solutions using raw and calcinated dolomite, J. Hazard. Mater. B 128 (2006) 273–279.
[16] E. Oguz, B. Keskinler, Determination of adsorption capacity and thermodynamic parameters of the PAC used for Bomaplex Red CR-L dye removal, Colloids Surf. A 268 (2005) 124–130.
[17] A. Baran, E. Bıçak, S.H. Baysal, S. Önal, Comparative studies on the adsorption of Cr(VI) ions on to various sorbents, Bioresour. Technol. 98 (2007) 661–665.
[18] S. Sun, A. Wang, Adsorption kinetics of Cu(II) ions using *N,O*-carboxymethylchitosan, J. Hazard. Mater. 131 (2006) 103–111.
[19] E. Malkoc, Y. Nuhoglu, Fixed bed studies for the sorption of chromium(VI) onto tea factory waste, Chem. Eng. Sci. 61 (2006) 4363–4372.
[20] M. Dundar, C. Nuhoglu, Y. Nuhoglu, Biosorption of Cu(II) ions onto the litter of natural trembling poplar forest, J. Hazard. Mater. 151 (2008) 86–95.
[21] J.E. Wertz, J.R. Bolton, Electron spin resonance, Elementary Theory and Practical Applications, New York, 1972, p. 13.
[22] R.P. De Carvalho, J.R. Freitas, A.M. De Sousa, R.L. Moreira, M.V.B. Pinheiro, K. Krambrock, Biosorption of copper ions by dried leaves: chemical bonds and site symmetry, Hydrometallurgy 71 (2003) 277–283.
[23] R.P. De Carvalho, K.J. Guedes, M.V.B. Pinheiro, K. Krambrock, Biosorption of thallium by dried plant leaves studied by electron paramagnetic resonance and infrared spectroscopy, Hydrometallurgy 59 (2001) 407–412.
[24] K. Flogeac, E. Guillon, M. Aplincourt, Adsorption of several metal ions onto a model soil sample: equilibrium and EPR studies, J. Colloid Interface Sci. 286 (2005) 596–601.
[25] E. Buszman, B. Pilawa, M. Zdybel, S. Wilczynski, A. Gondzik, T. Witoszynska, T. Wilczok, EPR examination of Zn^{2+} and Cu^{2+} binding by pigmented soil fungi. Cladosporium cladosporioides, Sci. Total Environ. 363 (2006) 195–205.
[26] A.H. Hawari, C.N. Mulligan, Biosorption of lead(II), cadmium(II), copper(II) and nickel(II) by anaerobic granular biomass, Bioresour. Technol. 97 (2006) 692–700.
[27] A.S. Luna, A.C.A. Da Costa, C.A. Henriques, M.H. Herbst, Electron paramagnetic resonance and atomic absorption spectrometry as tools for the investiga-

tion of Cu(II) biosorption by *Sargassum filipendula*, Hydrometallurgy 86 (2007) 105–113.
[28] E. Malkoc, Y. Nuhoglu, Adsorption of chromium (IV) on Pomace—an olive oil industry waste: batch and column studies, J. Hazard. Mater. B138 (2006) 142–151.
[29] Y.-S. Ho, A.E. Ofomaja, Kinetic studies of copper ion adsorption on palm kernel fibre, J. Hazard. Mater. B 137 (2007) 1796–1802.
[30] X.L.D. Xu, C.L. Tan, X.K. Chen, Wang, Adsorption of Pb(II) from aqueous solution to MX-80 Bentonite: effect of pH, ionic strength, foreign ions and temperature, Appl. Clay Sci. 41 (2008) 37–46.
[31] A. Çabuk, T. Akar, S. Tunali, Ö. Tabak, Biosorption characteristics of *Bacillus* sp. ATS-2 immobilized in silicagel for removal of Pb(II), J. Hazard. Mater. 136 (2006) 317–323.